



Simulating water uptake in the root zone with a microscopic-scale model of root extraction

Erwan Personne, Alain Perrier, Andrée Tuzet

► To cite this version:

Erwan Personne, Alain Perrier, Andrée Tuzet. Simulating water uptake in the root zone with a microscopic-scale model of root extraction. *Agronomie*, 2003, 23 (2), pp.153-168. 10.1051/agro:2002081 . hal-00886170

HAL Id: hal-00886170

<https://hal.science/hal-00886170>

Submitted on 11 May 2020

HAL is a multi-disciplinary open access archive for the deposit and dissemination of scientific research documents, whether they are published or not. The documents may come from teaching and research institutions in France or abroad, or from public or private research centers.

L'archive ouverte pluridisciplinaire **HAL**, est destinée au dépôt et à la diffusion de documents scientifiques de niveau recherche, publiés ou non, émanant des établissements d'enseignement et de recherche français ou étrangers, des laboratoires publics ou privés.

Simulating water uptake in the root zone with a microscopic-scale model of root extraction

Erwan PERSONNE*, Alain PERRIER**, André TUZET***

UMR Environnement et Grandes Cultures, INRA-INA PG, 78850 Thiverval Grignon, France

(Received 14 August 2001; revised 17 December 2001; accepted 4 June 2002)

Abstract – Root water uptake is a key element for analysing the evolution of soil water content, which regulates crop transpiration. Our objective was to design a model taking into account the vertical water redistribution and the root water uptake in order to assess the regulation of plant transpiration induced by the effective soil water availability. To do so, the root water uptake is described with a microscopic-scale model integrated within a classical model of vertical water redistribution. For root water uptake, the root water potential, leading the water transfer from soil to roots, is calculated in order to satisfy the climatic demand... By coupling the microscopic and macroscopic approaches to soil water transfer, the regulation of transpiration can be directly linked to soil hydraulic properties and to effective soil water availability: the numerical model is applied to simulate soil water movement with root water uptake, and simulation results are compared with a series of findings on plant functioning obtained by previous work. Qualitatively, simulated transpiration in response to the soil water content is reasonably consistent with the description of crop behaviour in drying soils and in soil with vertical water heterogeneity. The results are also compared with experimental results in order to evaluate the usefulness of this model: with conventional measurements under field conditions, the prediction of water balance evolution is rather consistent with experimental results.

model / root water uptake / soil-root transfer / transpiration / water

Résumé – **Simulation du prélèvement racinaire sur l'ensemble du système racinaire.** Le prélèvement racinaire d'eau par les plantes est le point-clé pour l'analyse de l'évolution du contenu en eau du sol, lequel régit la transpiration des cultures. Notre objectif est de concevoir un modèle qui prenne en compte à la fois la redistribution verticale de l'eau dans le sol et à la fois le prélèvement racinaire pour évaluer les régulations de la plante induites par la disponibilité de l'eau du sol. Pour cela, le prélèvement racinaire qui est évalué par un modèle d'extraction racinaire décrivant les transferts sol-racine à l'échelle microscopique est couplé à un modèle de redistribution verticale de l'eau dans le sol. Grâce à ce couplage entre une approche microscopique et une approche macroscopique, la régulation de la transpiration est directement reliée aux propriétés de transfert d'eau du sol et à la disponibilité effective de l'eau pour le système racinaire. Les résultats des simulations sont mis en parallèle avec un ensemble de résultats expérimentaux caractérisant les réponses des plantes à une phase de dessèchement du sol. Qualitativement, les comportements de la plante vus sous l'angle de l'eau sont reproduits de manière satisfaisante pour un sol s'asséchant et pour un sol ayant un profil vertical d'humidité hétérogène. Les résultats du modèle sont également comparés avec des résultats expérimentaux obtenus dans les conditions naturelles. A partir de mesures classiques réalisées aux champs, l'évolution du bilan d'eau modélisée est très comparable à celle mesurée.

modèle / prélèvement racinaire / transfert sol-racine / transpiration / eau

1. INTRODUCTION

Some models of water transfer in the soil-plant-atmosphere continuum (SPAC) have been developed in order to improve our understanding of plant behaviour in the environment. The major difficulty of these models is in estimating effective soil

water availability for the plant, which is a fundamental limiting factor of plant transpiration. In this context, these models have been developed to simulate the water budget and water movement in soil from two approaches to predicting root extraction: (i) models describing the vertical water dynamic in soil and including a "sink term" to represent root

Communicated by Serge Rambal (Montpellier, France)

* Correspondence and reprints
erwan@bcgn.grignon.inra.fr
** perrier@inapg.inra.fr
*** tuzet@bcgn.grignon.inra.fr

water uptake over each representative volume of soil, and (ii) models trying to explain the water soil-root transfer of each individual root.

Most often, the first type of model takes into account the vertical dynamic of water using Darcy-Richard's equation, and introduce an extraction function. This extraction function notably depends on transpiration rate, soil moisture diffusivity and root distribution [31, 53, 80] or depends on the gap between root water potential and soil water potential and on soil-root resistance [9, 38, 42]. These "macroscopic" models have generally been used for estimating water crop management [1, 30, 56, 86, 93]. Nevertheless, they cannot explain the diurnal variation in water soil content in the vicinity of the roots, which is an important process in plant regulation [29, 83, 88, 90, 100].

The second type of model is used to assess the impacts of factors affecting water uptake [16, 41, 50, 52, 84]. Formerly, this type of model, generally based on Gardner's approach [33, 42], did not take into account vertical water transport because radial transfer was considered predominant. Recent work has designed detailed models of the root system with root system architecture [20, 64], its hydraulics [22, 59, 87, 96] or integrating soil heterogeneity [47]. Some models in 2 or 3D have been developed to evaluate water transfer either in the plant or in the soil (see Pagès et al. 1998, for a recent review of the knowledge on root water uptake and on modelling it [63]). These works try to take into account drying soil around the roots and examine soil-root resistance in detail. They identify soil hydraulic properties, distribution of the root system [90] and root growth [15] as major factors of the soil water availability. Henceforth, taking into account the inner radial and axial resistance of roots, the research examines the physiological characteristics of the root segment on the centimetre scale in order to understand the activity of the roots [23, 61, 99]. However, these various approaches seem to be as yet non-operational for studies under natural or laboratory conditions either because water redistribution along the vertical axis is not taken into account, as has been the case for Gardner's type, or because the full coupling of the plants and the soil has not been achieved.

In this paper, a model of vertical water redistribution integrating water transfer from soil to roots is proposed. This model combines the two approaches: it describes vertical water transfer according to Darcy's law and it reproduces the soil-root system as many short cylinders representing the roots in horizontal layers of soil. Root water uptake is described on the basis of water transfer from soil to roots according to Gardner's approach. This combination of a microscopic model and a vertical soil water transfer model avoids the use of an empirical root extraction term which considers only spatial averages of soil water potential around the roots and takes no account of the increase in matric suction in the vicinity of the roots. It evaluates effective soil water availability from soil hydraulic properties. It is the first step before introducing the biological mechanisms of plant regulation into a model calculating water exchanges at the soil-plant-atmosphere interface.

We therefore examine in this paper the relevance of the results simulated by the model and the interpretations that can be proposed about soil-root resistance, water availability for the plant induced by the soil properties and therefore the regulation of transpiration by the soil.

2. MATERIALS AND METHODS

2.1. Theory and model for water transfer in soil

2.1.1. Basic principles for soil water transfer

Darcy's law describes the flow of an incompressible fluid in a homogeneous, rigid and isotropic porous medium. So, combining Darcy's law and the conservation equation [Eq. (1)] leads to soil water distribution in space and time given by the solution of Richard's equation [76]:

$$\frac{\partial \theta_v}{\partial t} = \nabla q \quad (1)$$

where t is time (s), θ_v the volumetric water content ($\text{m}^3 \cdot \text{m}^{-3}$), q the water flux density ($\text{m} \cdot \text{s}^{-1}$) and ∇ the vector differential operator in space.

Richard's equation can be written in general terms as:

$$\frac{\partial \theta_v}{\partial t} = \nabla \cdot [K \cdot (\nabla H)] \quad (2)$$

$H(m)$ is the total soil-water pressure head equal to Ψ_{-z} , $\Psi(m)$ being the matric soil-water pressure head and $z(m)$ the depth. K is hydraulic water conductivity ($\text{m} \cdot \text{s}^{-1}$), which depends greatly on the matric soil-water potential.

For reasons of simplification, contributions of heads to q , such as those due to solute concentration and coupling with temperature, are assumed to be negligible for this first work. So, in one dimension, along a vertical axis z , Richard's equation expressed in a "z-based form" [14] makes it possible to examine water potential dynamic:

$$C(\Psi) \cdot \frac{\partial \Psi}{\partial t} = \frac{\partial}{\partial z} \left\{ K(\Psi) \cdot \left(\frac{\partial \Psi}{\partial z} - 1 \right) \right\}, \quad (3)$$

where $C(\Psi) = \frac{\partial \theta}{\partial \Psi}$ is soil-water capacity (m^{-1}).

A complete numerical description of the redistribution process requires solving the unsaturated flow equation by numerical procedures explained in appendix A. The vertical space is divided into n_v horizontal layers and the boundary conditions at the bottom and on the soil surface can be chosen according to the environmental conditions (presence of groundwater, impermeable soil, rainfall, evaporation, etc.).

2.1.2. Soil-root transfer

Since we want to take the water uptake by the root system into account, we describe soil-root water transfer as a radial water flow from the soil to each section of the root surface. This approach is similar to the single root approach which was first developed by Gardner [33].

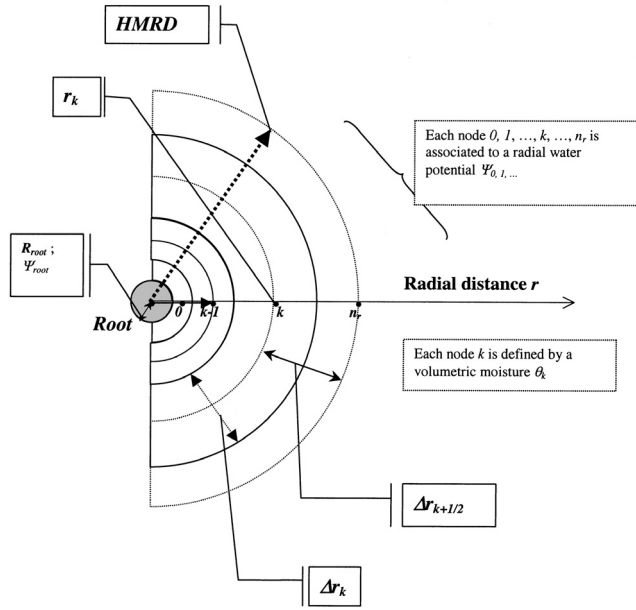


Figure 1. Schematic discretisation of a finite difference grid system for soil-root transfer. This representation of the space grid shows the different quantities that are used for the numerical resolution of radial transfer.

For an axial symmetric root with uniform water-absorbing properties, equation (2) leads to

$$C(\psi) \cdot \frac{\partial \psi}{\partial t} = \frac{\partial}{\partial r} \left\{ K(\psi) \cdot \frac{\partial \psi}{\partial r} \right\} + \frac{K(\psi)}{r} \cdot \frac{\partial \psi}{\partial r} \quad (4)$$

where r is the radial distance from the root axis. For soil-root transfer, this equation is confined between the soil-root interface [$r = R_{root}$; R_{root} being the root radius] and the half mean distance between each root ($r = HMRD$; $HMRD$ being the radius of the outer boundary of the soil cylinder located midway between adjacent roots). This distance depends on root length density ρ_{root} in $\text{m} \cdot \text{m}^{-3}$ ($HMRD = 1/\sqrt{\pi \rho_{root}}$), which is itself dependent on the distribution of the root system ($\rho_{root} = \rho_{root}(z)$). This approach to the description of soil water potential dynamic around the roots is greatly dependent on the potential at the root interface ($\Psi_{root} = \Psi(r = R_{root})$). The water influx inside the roots, generated by this interface, is regarded as water contributing to plant water transfer and transpiration. In this first approach, root interface potential is equivalent to the water potential in the whole plant because it is assumed that radial resistance in the root tissue and axial resistance in the plant from roots to leaves does not affect water flow [11, 99]. So, the boundary conditions for equation (4) are the Dirichlet condition with Ψ_{root} set at $r = R_{root}$ and the Neumann condition for the outer boundary of the soil cylinder with $\partial \Psi / \partial r = 0$ at $r = HMRD$. Precise details of the numerical resolution of the radial system are given in appendix A and Figure 1.

2.1.3. Coupling between radial and vertical transfer

The radial approach to explaining soil water uptake is combined with the vertical processes of soil water transfer (see

Fig. 2). Sequential coupling between water extraction and vertical water transport is used. For each horizontal layer describing the vertical space grid, the model of radial soil-root transfer is solved. Each horizontal layer k is characterised by a half mean root distance ($HMRD(z_k)$), a root radius (R_{root}) and a radial soil water profile. Because of the discretisation of the radial soil-space in the horizontal layers, vertical transfer is calculated from mean moisture expressed at each depth z_k . The hypothesis is to choose for this mean value, the integrated moisture $\bar{\theta}_k$ resulting from the radial space grid:

$$\bar{\theta}_k = \frac{1}{HMRD(z_k)^2 - R_{root}^2} \cdot \sum_{i=0}^{n_r} \theta_i^k \cdot 2 \cdot r_i \cdot \Delta r_i. \quad (5)$$

At depth z_k , θ_i^k is the volumetric moisture for node i of the radial space grid, r_i and Δr_i are distance r and thickness Δr of the radial node i : $HMRD(z_k)$ is the half mean root distance between roots at this depth, dependent on the depth because of varying root length density with depth. n_r is the number of radial layers in the radial space grid (see Fig. 1 for the description of the radial space grid).

The model uses several sequential resolutions in one time step Δt . Firstly, the model calculates radial diffusion in each horizontal layer k in order to simulate root absorption (Eq. (4)). Then, from equation (5), the mean moisture of layer k is calculated, making it possible to solve vertical water transport (Eq. (3), Fig. 2). In the last step, to conclude the processes of the time interval Δt , the redistribution of the vertical transfer inside the radial grid-spaces is carried out with simple redistribution proportional to the surface of the radial layers. This leads to the equation:

$$(\theta_i^k)^{t+\Delta t} = \theta_i^k + \Delta \theta_k \quad (6)$$

with $\Delta \theta_k$ being moisture variation in the horizontal layer resulting from vertical transfer during Δt .

2.2. Root water extraction in response to climatic demand

2.2.1. General ideas to integrate plant behaviour

The evapotranspiration flow of a plant is considered to depend on the atmospheric environment and on stomatal aperture. We consider, as mentioned in Lafolie et al. (1991), that the plant adjusts its root water potential to take up the amount of water equal to the transpirative demand. This transpirative demand is given by the maximal transpiration called TM (in $\text{kg} \cdot \text{m}^{-2} \cdot \text{s}^{-1}$), which only depends on the climatic demand, the structure of the cover (leaf-area index and height) and minimal stomatal resistance [54, 68].

The principle of this model is to minimise the difference between maximal transpiration and the amount of water taken up by the roots, which is driven by the root water potential. The conventional hypotheses on water transfer through the root are summed up in these different points:

1. The conceptual model is based on optimising root water potential in order to satisfy the maximal transpiration. This

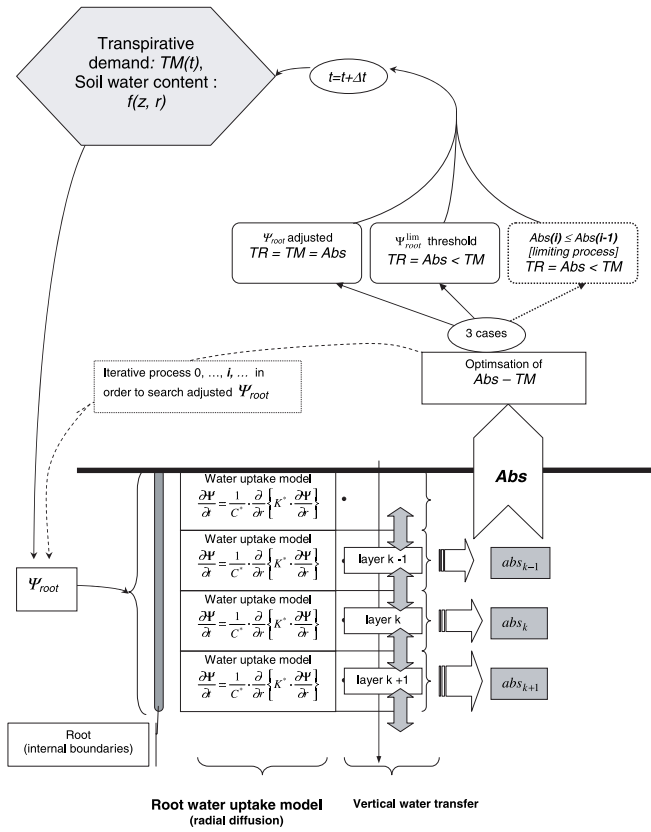


Figure 2. Schematic diagram of the combined radial and vertical transfer. Algorithm to optimise root water uptake and the transpirative demand is not detailed. TM is the maximal transpiration imposed by climatic demand, TR and Abs are real transpiration and total water absorption of the plant. abs_k is root water absorption in the soil layer k and Ψ_{root} is the water potential of the root which directs the water transfer from soil to roots.

maximal transpiration is assumed to be unrelated to the root water potential and soil water potential.

2. Root water potential is homogeneous in the root system. All roots have the same potential, which is the driving force behind the extraction of water from all horizontal soil layers. This approach makes it possible to avoid integrating internal plant resistances that are often lower than soil-root resistance or stomatal resistance.
3. Since there is some evidence that the release of water from root to soil is negligible for most common crops [21, 60], the flow from root to soil is always zero. If some roots have a higher potential than the surrounding soil, the conductivity of the soil root interface is set at zero because it has been shown that a hydraulic barrier inside the root appears in order to avoid water transfer from root to soil.
4. The contribution of plant-tissue water storage to transpiration is not incorporated into the model; this work should be carried out in the future so as to improve the model [69].

According to hypotheses 2 and 3, if the climatic demand is zero or negative, such as during the night or a rainfall period,

the roots adjust their potential to the higher potential in the soil.

2.2.2. Optimisation of the root water potential

For the calculations of root water potential, it is assumed that the plant continuously adjusts its inner potential (Ψ_{root}) so as to take up as much as possible of the amount of water corresponding to the maximal transpiration TM [47]. With this hypothesis, for each time interval Δt , the problem consists of finding the root water potential that minimises the difference between maximal transpiration and water uptake by the root system. So, with the hypothesis of non-interaction between root water potential and stomatal regulation (hypothesis 1), the amount of extracted water is evaluated by the whole set of radial models integrated into the horizontal layers (Fig. 2). Initialisation of the searching process begins from an initial value Ψ_{root} which is gradually decreased from the higher water potential in the soil until Ψ_{root} allows the adjusted water quantity TM to be extracted (see the algorithm of Fig. 2).

For each horizontal layer k at z_k of thickness Δz_k , the radial model of water uptake gives an extracted water quantity abs_k (Eq. (7), in $\text{kg} \cdot \text{m}^{-2} \cdot \text{s}^{-1}$) according to the water loss ($[\phi_k]^{\Delta t}$) of the radial system representative of the roots (Eq. (8)) and according to the root length in this layer k :

$$abs_k = \rho_{Root}(z_k) \times \Delta z_k \times [\phi_k]^{\Delta t} \quad (7)$$

with

$$[\phi_k]^{\Delta t} = \frac{Q_k^{t_j+1} - Q_k^{t_j}}{\Delta t} \quad (8)$$

$Q_k^{t_j}$ (in kg of water per length of root) being the amount of water surrounding the radial system in the horizontal layer k and at time t_j . Δt is the time step between t_j and t_{j+1} .

Water extracted by the plants for soil surface unity (Abs in $\text{kg} \cdot \text{m}^{-2} \cdot \text{s}^{-1}$) during the time interval Δt is given by equation (9).

$$Abs = \sum_{k=0}^{n_v} abs_k \quad (9)$$

The optimisation of root water potential consists of finding the value of Ψ_{root} inducing equality between root extraction (Abs) and maximal transpirationTM (Fig. 2). Convergence to the adjusted Ψ_{root} is reached by an algorithm which gradually decreases Ψ_{root} . Convergence is satisfied when the fixed criterion $\varepsilon_{adj} \left[\frac{|Abs - MT|}{MT} \leq \varepsilon_{adj} \right]$ is obtained.

2.2.3. Limiting flux and consequences for real transpiration

Root water potential must be at suction lower than the soil water potential surrounding the root for soil water to be taken up by the roots within each horizontal layer. The difference between potential in the root (Ψ_{root}) and soil water potential increases for a given uptake water flux as the soil dries because of the high non-linearity between hydraulic conductivity and soil water content. In the model, as long as the plant can

Table I. Fitted soil characteristics and hydrodynamic properties for the pressure head-water content relationship and the conductivity-water content relationship [13].

Soil	θ_s $\text{m}^3 \cdot \text{m}^{-3}$	θ_r $\text{m}^3 \cdot \text{m}^{-3}$	Ks $\text{m} \cdot \text{s}^{-1}$	α m^{-1}	n	p
Loam	0.43	0.078	2.89×10^{-6}	3.6	1.56	0.5
Silt	0.46	0.034	7.00×10^{-7}	1.6	1.37	0.5
Clay	0.38	0.068	5.80×10^{-8}	0.8	1.09	0.5

decrease its potential to maintain maximal transpiration, water is considered to be available to the plant and no stomatal regulation occurs.

With the hypothesis that the contribution of water-tissue storage to transpiration is low (water uptake by the roots = real transpiration; hypothesis 4) and that the reduction in transpiration by specific regulation of the plant does not occur, transpiration could be reduced directly by soil water transfer surrounding the root and by the soil-root interface.

In the light of this preamble, two processes appear to explain the reduction in water uptake and therefore real transpiration.

Firstly, the formation of intense soil drying in the vicinity of the roots creates a hydraulic barrier around the roots. This hydraulic barrier appears because soil hydraulic conductivity tends towards zero when the potential at the soil-root interface is very low. In dry soil, a limiting flux therefore appears, considering the decrease in hydraulic conductivity around the roots. This leads to real transpiration that is lower than maximal transpiration ($Abs = TR$). In order to explain and confirm the existence of such a limiting flux, the appendix B-a analytically demonstrates it in steady state. Determining the limiting flux by numerically solving the radial transfer model (appendix B-b) thus introduces a reduction in transpiration inherent in the soil-root transfer capacity. Consequently, this limiting uptake which induces real transpiration, that is lower than maximal transpiration, should explain the corresponding stomatal regulation due to the soil-root environment.

Secondly, biological regulation is introduced with a threshold value for root water potential Ψ_{root}^{lim} [30]. This threshold value is comparable to the wilting point which is specific to the plant. It is assumed that the plant cannot withstand a water potential under this value without damage. Consequently, it is assumed that the plant is able to reduce the stomatal aperture and adjust it to keep water potential at the value of Ψ_{root}^{lim} . Actual transpiration therefore becomes lower than the maximal transpiration imposed.

In this approach, the regulation of real transpiration is modelled in two ways: soil regulation induced by soil-root transfer and independent biological regulation generated by the stomatal response due to the effects of threshold root water potential on water transfer in the plant. This second way of reducing real transpiration can overlap with the limiting flux in order to impose stomatal regulation.

3. RESULTS

The results of the simulations are divided into two sections. Firstly, from reference and arbitrary but realistic situations,

specific outputs of this model are compared with the literature in order to show that the model was better at explaining root water uptake and its consequences on transpiration regulation. This makes it possible to test the realism of this approach integrating mechanistic soil water transfer. Secondly, the model is used to predict the evolution of the soil water balance on the field scale in order to verify its usefulness.

3.1. Analysis of reference simulations

3.1.1. Initial conditions and parameters used as a basis for simulations

For reference outputs, calculations are carried out for a climatic demand corresponding to maximal transpiration TM following sinusoidal distribution between 6h00 and 18h00. The maximum of TM reaches $0.73 \text{ mm} \cdot \text{h}^{-1}$ at 12h00 ($500 \text{ W} \cdot \text{m}^{-2}$), which was a mean condition during our experiment on grass in Niger and described in Personne [70]. During the night, maximal transpiration is equal to $0.01 \text{ mm} \cdot \text{h}^{-1}$.

For general considerations, simulations are performed with three contrasting soil types: loam, silt and clay. The relationships between matric soil and water content and also with the soil conductivity are obtained for each soil type with the analytical expressions proposed by van Genuchten [94]:

$$\frac{\theta - \theta_r}{\theta_s - \theta_r} = \left[1 + |\alpha \Psi|^n \right]^m \quad (10)$$

and

$$K(\Psi) = Ks \cdot \frac{\left\{ \left[1 + |\alpha \Psi|^n \right]^m - |\alpha \Psi|^{n-1} \right\}^2}{\left[1 + |\alpha \Psi|^n \right]^{m(p+2)}} \quad (11)$$

where θ_s and θ_r are the saturated and residual volumetric water contents ($\text{m}^3 \cdot \text{m}^{-3}$), Ks is saturated hydraulic conductivity ($\text{m} \cdot \text{s}^{-1}$), α (m^{-1}) and n are fitted parameters for the soil characteristics with $m = 1 - 1/n$ and p is a parameter that can be set at 0.5 [55]. The parameters introduced to describe the hydrodynamic characteristics of these typical soils are found in Carsel and Parrish [13] (Tab. I). Figure 3 represents the relationships used for each soil.

For the plant, the model is performed with typical parameters of a herbaceous canopy in Niger. We have chosen to introduce a constant root length density of $1250 \text{ m} \cdot \text{m}^{-3}$ (root length per unit soil volume) in a soil 0.5 metres deep. The diameter of each root is 0.5 mm. The wilting point for the plant is given for a root threshold potential of -160 m ($\Psi_{root}^{lim} = -1.6 \text{ MPa}$ = root water potential below which it is considered that the root cannot decrease without biological damage).

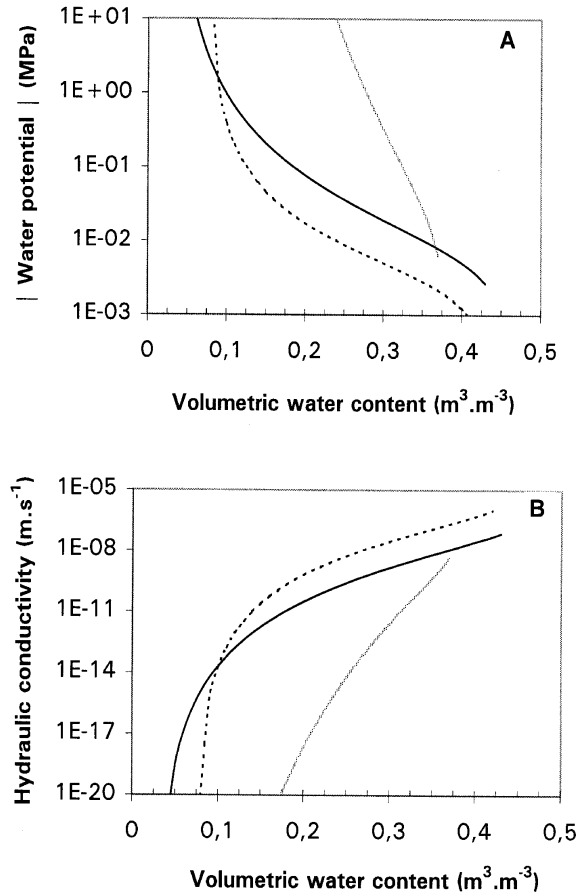


Figure 3. Presentation of the hydrodynamic characteristics of the three soils used in the simulations. Dashed lines represent the loamy soil, solid lines the silt soil, and grey lines the clay soil. (A) pressure head-water content relationships. (B) water content-hydraulic conductivity relationships.

For numerical processing, the following conditions are introduced: the vertical soil profile is divided into 7 nodes ($n_v = 6$). The numerical grid to describe water soil transfer along the radial axis is divided into 15 equidistant nodes ($n_r = 14$). These discretisations calculate water transfer with a minimum of numerical errors [70]. The convergence of the simulations is considered satisfactory for the convergence criterion ε_c of 0.0001. Root water potential is assumed to be optimised if the difference between water uptake and TM during each time step t satisfies the convergence criterion ε_{adj} . The parameters of the model are summed up in Table II.

Table II. Parameters incorporated in the model for the simulations. ΔM corresponds to the maximal error of total mass balance due to numerical resolution, $\Delta t(\text{iteration } 0)$ corresponds to the initial time-step used for the calculation and $\Delta t(\text{mini})$ to the minimal time-step after which there is no further decrease in the time-step.

Parameters	n_v	n_r	Convergence ε_c	Optimisation ε_{adj}	ΔM (mass bal.) (in %)	Δt (iteration 0) (in s)	$\Delta t(\text{mini})$ (in s)	$\Psi_{\text{root}}^{\text{lim}}$ (in MPa)
	6	14	10^{-4}	10^{-4}	10^{-5}	56.25	7.03125	-1.6

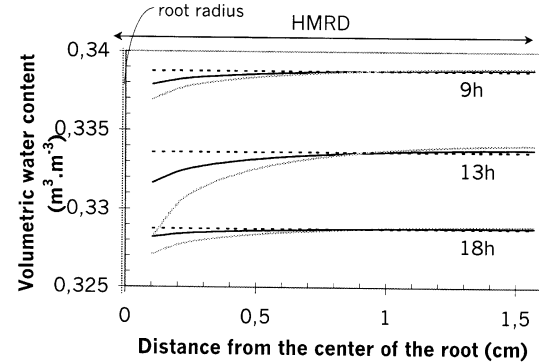


Figure 4. Soil water content depending on the distance of the root at various times. The initial water content is $0.34 \text{ m}^3 \cdot \text{m}^{-3}$ and the need for root water uptake corresponds to the daily cycle of transpirative demand (sinusoidal form between 6 h and 18 h and maximum equal to 0.73 mm/h at 12 h) [dashed lines represent the loamy soil, solid lines the silt soil and dotted grey lines the clay soil].

The choice of this set of inputs integrates the plant in a realistic environment and the three types of soil used makes it possible to understand the range of plant responses to soils with different transfer characteristics.

3.1.2. Results for cylindrical root water uptake

3.1.2.1. Resulting gradients around the roots

The results for different types of soil with the same initial soil moisture conditions ($0.34 \text{ m}^3 \cdot \text{m}^{-3}$) are presented to compare the formation of gradients around the roots. The initial conditions can be considered as relatively wet because of the high water potentials. Figure 4 shows the evolution of the soil moisture surrounding the roots at depth $z = 0.3 \text{ m}$ for each soil and at 3 different times of the day. The formation of a “dry” zone in the vicinity of the roots in clay soil appears throughout the day. Around midday (13 h) the simulation with the clay soil reveals the highest potential drop between the soil near the root and the soil at the half mean distance between the roots. For loamy soil, no “dry zone” appears around an absorbing root. The situation for silty soil is intermediate. Because of the diurnal cycle of the climatic demand inducing water uptake, the model reproduces greater dryness around the roots during high demand (13 h) than during low demand (9 h). In fact, the gradients are very small in the case of soils with high conductivity levels such as loam and in the case of moist soil, because soil water transfer occurs very rapidly.

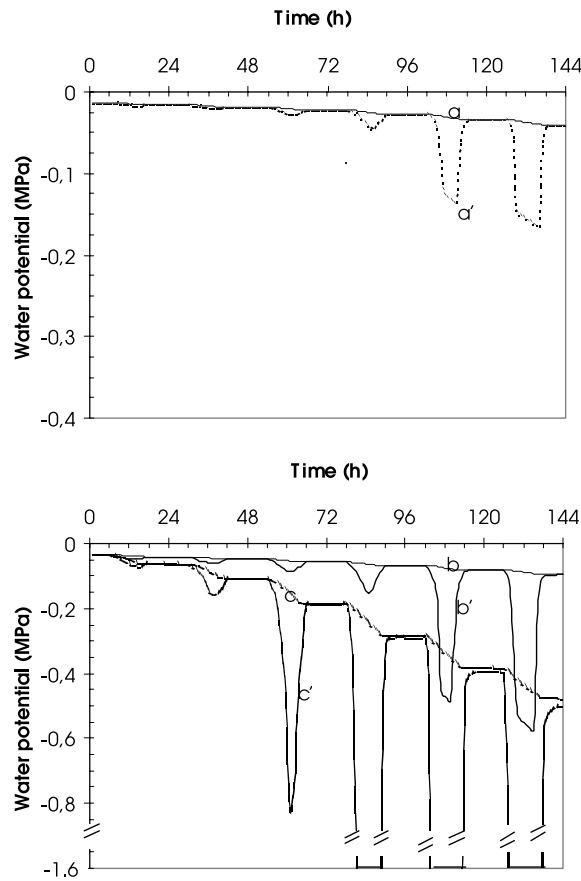


Figure 5. Root and mean soil water potential vs. time during a few days of drying out via root absorption. Curves *a* and *a'* correspond, respectively, to the mean soil water potential [thin dashed line] and root water potential [thick dashed line] in loamy soil, *b* and *b'* to the mean soil water potential [thin solid line] and root water potential [thick solid line] in silty soil, and *c* and *c'* to the mean soil water potential [thin grey line] and root water potential [thick grey line] in clay soil.

3.1.2.2. Consequences for root water potential and predawn root water potential

Soil-root water transfer in response to transpiration demand introduces a dynamic root water potential. Figure 5 shows the evolution of the root water potential during a drying period (6 days) for the three soil types initially at the same soil water potential (-0.03 MPa). The mean soil water potential is obtained from the mean water moisture calculated throughout the entire soil depth ($0-0.5$ m). The relationship $\psi = f(\theta)$ [Eq. (10)] gives a mean reference for the water status in the soil. Figure 5 thus represents the diurnal cycle of the root water potentials (curves *a'*, *b'* and *c'*) and the slight decrease in soil water potential during the day related to water loss by root uptake (curves *a*, *b* and *c*). These results reveal that the diurnal cycle of root water potential is very sensitive to the combination of climatic demand [81], water content in the soil [77] and type of soil: during the day, the potential gradients between soil and roots increase whereas, during the

night, these gradients decrease to return to equilibrium [44]. The minimal root water potential of each day is lower and lower because a drying soil is correlated to a decrease in soil hydraulic conductivity [97]. It is worth noting that gradients between root and soil water potential are very different, depending on the type of soil.

In these examples, predawn root water potential is comparable with the soil water potential given by the mean soil water content. During the night, because of the very low transpirative demand, the root water potential tends towards the mean soil water potential. In the situations expounded, predawn root water potential is representative of the soil water status. This conventional hypothesis of equilibrium between the water potential of soil and the potential of the plant during the night is dependent on the time necessary to tend towards equilibrium, which is correlated to the soil water transfer abilities, i.e. to the type of soil and to soil moisture. For example, at the end of the simulation for clay soil, we noted that the return to equilibrium occurred less rapidly than during the previous days. Of course, for dry clay soil, the root water potential at the beginning of each day does not correspond to the mean soil water potential because night-time is often not long enough to return to equilibrium by passive diffusion.

3.1.2.3. Consequences of the reduction in water extraction for plant regulation

The main interest of this model is that it examines plant regulation induced by water content in the soil. From the simulations generated in the previous section, the outputs of real transpiration (*TR*) are examined for the three soil types initially at a soil water potential of -0.03 MPa (Fig. 6). According to the soil water content, the results presented first outline the general case in which the decrease in root water potential can maintain the transpirative demand because water availability is high enough to uptake water from the diurnal and temporary decrease in root water potential (see the first days for the three types of soil where real transpiration coincides with maximal transpiration). They also outline the cases where water extraction by roots cannot satisfy maximal transpiration:

(i) The reduction results from the limiting flux caused by the soil drying around the root. From the fifth day (Fig. 6), for silt soil, transpiration begins to reduce without reaching the limit value ψ_{root}^{lim} set at -1.6 MPa (see in parallel Fig. 5). This reduction in transpiration is due to the fact that the plant is unable to extract more water even if the root water potential decreases. (ii) The second case corresponds to a limit value ψ_{root}^{lim} which is reached by the root water potential. The large amplitude occurring for water uptake in dry soils can generate a root water potential that decreases down to the value ψ_{root}^{lim} (clay soil after 80 hours; day 4, see Fig. 5). This approach with a threshold value is often incorporated into models [31] to explain the physiological limitations of the plants in dry soils by using an integral value corresponding to a wilting point. This threshold induces a given water influx in the plant and associated stomatal regulation because of a supposedly conservative flux through the plant (stomatal closure fits so

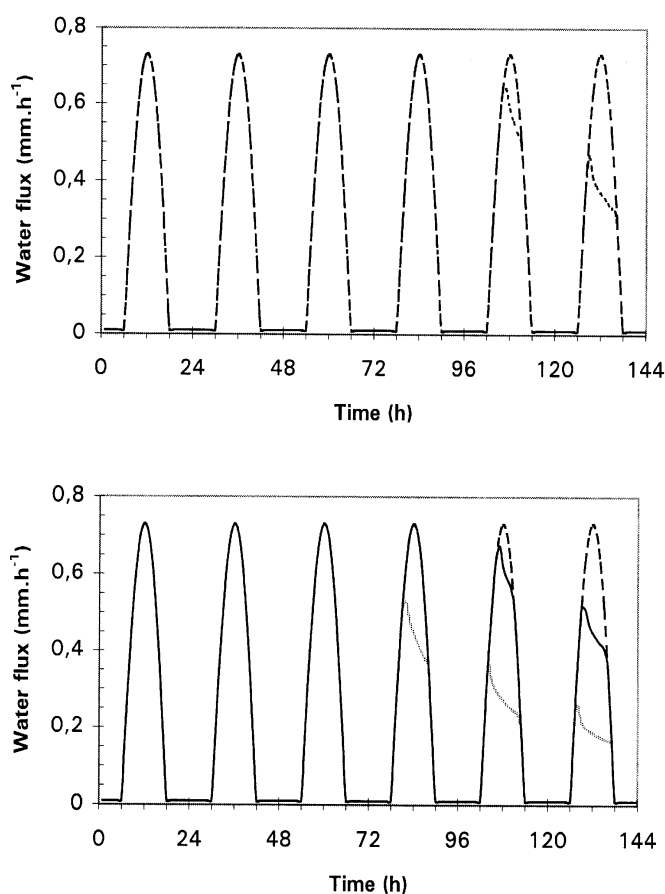


Figure 6. Real transpiration and maximal transpiration vs. time in response to drying soil (see above). Transpirative demand (TM) is represented by the thick dashed line. Thin lines correspond to real transpiration (TR) in response to water extraction ability (dotted line for response in loamy soil, thin solid line in silt soil and grey line in clay soil).

that the root water potential stays at this value in order to avoid physiological damage).

3.1.3. Cylindrical and vertical coupling model

By coupling vertical transfer and radial transfer, the model takes into account the impact of root distribution according to the depth, the impact of the various types of soil present in the soil explored by the roots and the impact of vertical water redistribution on root water uptake. For example, in order to show the impact of water profile on water uptake, simulations are carried out with two different initial soil water profiles with silt soil (see Fig. 7). The results confirm that the vertical water profile must be taken into account in order to explain plant behaviour in a cultivated soil subject to heterogeneity in the situations concerning the soil and the climate.

Owing to the influence of the vertical profile on plant responses (TR), the evolution of the root water potential and the mean soil water potential resulting from the two simulations with different initial vertical profiles is presented

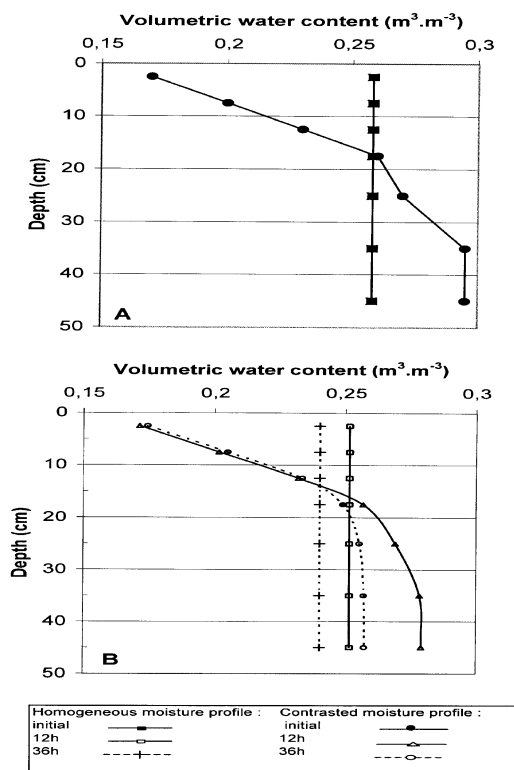


Figure 7. (A) Initial vertical moisture profiles introduced in the simulations (homogeneous and contrasting vertical profile). (B) Vertical moisture profiles from two different initial conditions at 12 h (solid lines) and 36 h (dashed lines) during drying period. Results from the initial homogeneous profile are presented with square and cross symbols, results from the initial contrasting profile with triangle and rhomb symbols.

in Figure 8. The mean soil water potential is the same for the two cases because it results from the total water content from 0–0.5 m and submits to the same climatic demand, but the root water potential is different: (i) from the initial homogeneous profile, the root water potential decreases to -0.045 MPa at 14 h and -0.057 MPa at 38 h and returns to mean soil water potential during the night. The predawn root water potential can be considered representative of the mean soil water potential. (i) From the contrasting initial profile, the simulation reveals a higher root water potential than the mean soil water potential (-0.033 MPa at 14 h and -0.046 MPa at 38 h) and a return to equilibrium during the night that differs from the mean soil water potential.

3.2. Use of this approach under field conditions

Without being a point-by-point validation of the processes incorporated in the model, simulated results are compared with experimental results obtained from a field experiment. The model calculates the evolution of the soil water content from climatic forcing and parameters describing vegetation and soil hydraulic characteristics. It makes it possible to test the

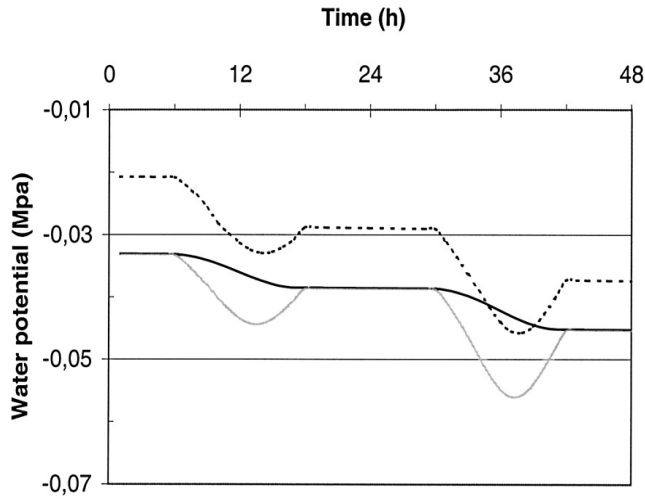


Figure 8. Evolution of the root and mean soil water potential over two days. Mean soil water potential is represented with solid, grey and dashed lines, respectively, indicating the evolution of the root water potential from the homogeneous vertical profile and from the initial contrasting vertical profile.

model on soil water balance evolution from standard measurements in the field.

3.2.1. Description of the field experiment

Data used are listed in the work of Personne (1998) and are the results of an experiment in Grignon in 1997 (Paris region). The soil is characterised by two varying layers of which the hydrodynamic properties are measured using the modified

Wind method [89] (see Tab. IV – for the soil parameters used). The crop is made up of wheat over 96% of the surface and of maize over the remaining 4% (a regular but sparse array of clumped maize plants [92]). The atmospheric model that calculates maximal transpiration is described in Personne (2001). For the simulation under natural conditions, the results presented are obtained from the initial soil moisture profile measured by gravimetry, from the real measured root profile which is assumed to be invariant during the time of the experiment (from $1500 \text{ m} \cdot \text{m}^{-3}$ near the surface to $0 \text{ m} \cdot \text{m}^{-3}$ at 1.5 metres deep) and from the discretisation of the vertical soil space in 13 nodes. Unlike the previous simulations, which examine the coherence of the results and the advantages of coupling the microscopic and macroscopic approaches, the simulations are performed with real soil, plant and atmospheric conditions. The cover structure (Leaf Area Index and height) are measured and prescribed within the model to take plant growth into account. So, boundary conditions for vertical water transfer are the gravitational flux (free drainage) in the lower boundary and the evaporation flux calculated by the atmospheric model for the soil surface.

3.2.2. Results

3.2.2.1. Soil water balance

The evolution of soil water content is given in Figure 9. During this period, soil water content regularly decreases due to the evapotranspiration of the crop. Only the considerable rainfall in mid-August contributed to the significant increase in the soil water content of the first soil metre. The figure therefore gives the measurements made using the gravimetric method, TDR system and the outputs of the simulation. The rather close agreement between the model and the

Table III. Description of the notations for the numerical discretisation.

$k = 1, \dots, n_v ; k = 1, \dots, n_r \rightarrow$	$\Delta z_k = (z_{k-1} - z_{k+1})/2$
$k = 0 \rightarrow$	$\Delta z_0 = 3/2 \times z_0$ vertical axis $\Delta r_0 = 2 \times (r_0 - R_{root})$ radial axis
$k = 0, \dots, n_v ; k = 0, \dots, n_r \rightarrow$	$\Delta z_{k \pm 1/2} = z_k - z_{k \pm 1}$
$j = 0, 1, \dots, n_t \rightarrow$	$\Delta t = t_{j+1} - t_j$

Table IV. Fitted soil characteristics and hydrodynamic properties for the pressure head-water content relationship and the conductivity-water content relationship during the experiment [70].

Soil	θ_S $\text{m}^3 \cdot \text{m}^{-3}$	θ_R $\text{m}^3 \cdot \text{m}^{-3}$	Ks $\text{m} \cdot \text{s}^{-1}$	α m^{-1}	n	p
Soil surface (0–30 cm)	0.401	0.002	1.08×10^{-6}	0.32	1.33	0.5
Soil under 30 cm depth (30–110 cm)	0.401	0.061	2.04×10^{-7}	3.14	1.125	0.5

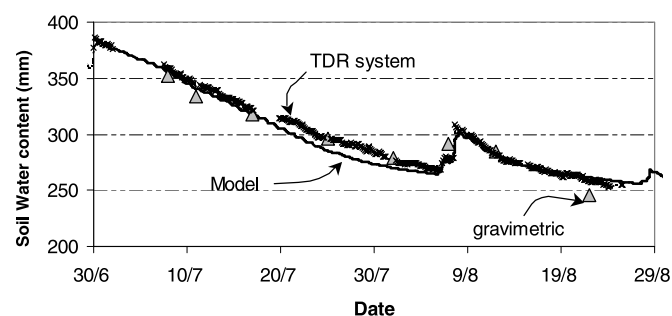


Figure 9. Soil water content evolution from the soil 1.1 metres deep. Results were obtained in the Paris Region in 1997 with wheat and maize crops [70, 71].

measurements can be emphasised because the differences remain below 15 mm for a soil water content higher than 250 mm.

3.2.2.2. Evolution of the vertical profile

Whereas the soil water content dynamic is relatively well reproduced, it is also interesting to examine the evolution of the soil moisture profiles because it improves how the zones of root water uptake are determined and makes it possible to experimentally verify the model specificity (root water uptake and vertical redistribution). Figure 10 therefore indicates the evolution of the simulated and measured soil water profile. The simulated evolution is very coherent with the experimental results. However, some differences appear near the soil surface. For the first centimetres of soil surface, soil evaporation and root water uptake overlap each other. It is well known that surface fluxes pose a lot of problems considering (i) the available energy at the soil surface and therefore partitioning between evaporation and transpiration, which is a key element for atmospheric models, (ii) soil vapour transfer, which is not taken into account although it is at this level (near the surface) that it occurs [66], and (iii) root water uptake in the first soil centimetres, for which knowledge is lacking.

4. DISCUSSION

To assess the quality of the model, (i) a parallel is drawn between each simulation result and the findings of some other experimental works, and (ii) a comparison between experimental results in the field and simulations is made. In a first step, the modelling is therefore tested to see if the integration of the basic process (coupling between the microscopic and macroscopic approaches) qualitatively reproduces plant functioning and if it could explain its regulation when subject to a drying period. In a second step, the model is assessed under field conditions in order to gauge its potentiality and functionality.

Why have we combined a microscopic approach with a macroscopic approach in this model? We think that the first step towards integrating the soil-plant function is understanding the influence of water transfer from the soil to the roots before taking into account the relevance in terms of

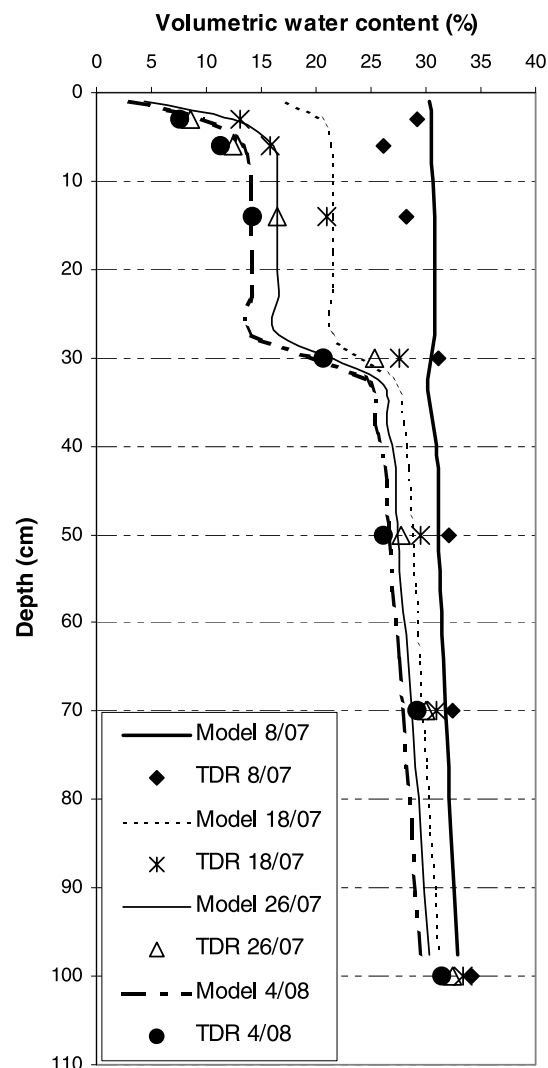


Figure 10. Simulated and measured soil water profile during the experiment in 1997.

physiological responses of plants to water availability. Moreover, taking soil-root transfer and vertical soil water redistribution into account appears necessary in order for the model to be useful under natural conditions.

Indeed, this model of water uptake in soil allows us to predict hydraulic failure in the vicinity of the roots, which could generate a reduction in transpiration. This is an improvement on the approaches to soil water uptake by roots because the modelling of soil-root transfer and the limiting flux appearing in the soil around the roots suggest an alternative to using a sink term in Richard's equation for vertical redistribution. Indeed, the sink terms empirically introduce root water uptake, and no decrease in soil water potential or hydraulic conductivity in the vicinity of the roots is reproduced, and yet it is often indicated that the soil-root interface is a key element of transfer in the soil-plant-atmosphere continuum [27, 46, 91, 100]. We emphasise that

no biological regulation is taken into account in this first approach: the potential impact of soil-root transfer on transpiration regulation can thus be examined in detail. Without the specific biological regulation linked to cavitation, plant capacitance and stomatal response to leaf water potential being introduced, it appears nevertheless that some points seem satisfactory to reproduce the functioning of plants in drying soil:

- It appears that some researchers distinguish between soil water availability, which only depends on the soil hydraulic properties, and soil water accessibility, which depends on the combination (i) of the ability of soil to transfer water towards the roots (“availability”) and (ii) soil exploration by the roots [6, 25]. In fact, the main objective of this work on root water uptake is to improve how soil-root resistance in the soil-plant-atmosphere is assessed and understood because it is often controversial. Indeed, some researchers have concluded that soil resistance has a major role in the SPAC [27, 34, 50, 100], while we have found some experimental work showing that the influence of soil-root transfer is negligible compared with water resistances in the plant [5, 56, 67, 74]. Like some varying models of water transport in SPAC [7, 16, 33, 50, 51, 84], hydrodynamic characteristics, the hydric status of the soil and soil exploration by the roots can be put forward to explain the conflicting results. Our results show varying behaviour according to the type of soil (i.e. Fig. 4 and Fig. 5). In fact, the properties of water transfer in soil and soil exploration should probably affect the plant transpiration directly. The formation of gradients around the roots has been demonstrated experimentally by some work [26, 36, 79]. Nye et al. [62] indicate that, as the soil matric potential drops, root water uptake exceeds the supply by mass flow and the soil dries out at the soil-root interface. Hamza and Aylmore [37] and Young [98] observed that the preferential drying around the roots does not extend far beyond the first 2 millimetres and focuses on transfer in the rhizosheath. The various existing results, however, present different findings on potential gradients and soil resistance which form around the roots. Our simulations confirm that the analysis of soil water transfer for root uptake is highly correlated to the hydrodynamic properties of the soil and to the intensity of root absorption (Fig. 4). The approach used therefore makes it possible to integrate these specific processes that are certainly crucial for plant regulation.
- As for the integration of plant functioning in the model, although the hypothesis of homogeneous root water potential is not realistic [81, 94], it has been shown in previous works that this simplification seems to be sufficient to determine the evolution of the water soil profile during root water uptake [57, 78], provided that the vertical redistribution of water in soil is well described. With the radial approach and the simplified hypothesis of plant functioning (see Sect. 2.2.1), when the soil dries, the progressive decrease in the root water potential is consistent with the evolution of the leaf water potential which has been studied previously by some authors [43, 45, 73, 77]: root water potential follows a diurnal/nocturnal cycle and the minimal values reached during the day are lower and lower. Moreover, the mean soil water potential

can be different from the predawn root water potential which has been confirmed by a number of experimental and modelling works (see [32, 47, 70, 79], for example): if the soil is wet, water diffusion around the roots during the night is fast-flowing enough to have equilibrium between soil water potential and root water potential. This is not the case for low water content, for which soil conductivity is not high enough to allow the return to water equilibrium during the night [47] (see Fig. 5). With radial and vertical coupling, the model resolves a major difficulty induced by the use of the radial approach alone. For example, results in this paper pointed out the consequences of wet deep horizontal layers on the water supply of plants: (i) the results in Figure 7-B and Figure 10 express relatively well the vertical variability in root water uptake which seems to be consistent with real plant functioning (plants extract soil water where it is most available [2, 58, 72, 75, 82]). (ii) The model emphasises that the interpretations concerning the predawn root water potential and its role as a stress indicator of the plant and the mean soil water content must be completed by knowledge of the vertical profile, since the predawn root water potential is more directly linked to the higher potential in soil than a mean water potential representative of the overall water content (Fig. 8) [2, 3, 8, 21].

It could be added that the knowledge of water transfer resistances in the soil-plant-atmosphere continuum, in particular soil-root resistance, should include phenomena such as root suberisation, root contraction during transpiration [28], or cavitation in conductive vessels [17, 85]. It must be emphasised that root shrinkage and the loss of hydraulic contact between the soil and the plant root [95] may substantially alter the results presented in this paper. Their influences would decrease the root water potential or should increase the differences between real transpiration and transpirative demand. Conversely, the mucilage and changes in soil characteristics due to root extraction [10, 19, 35] or the relationships between root growth and root extraction [15] are also phenomena that could greatly influence the results by adaptation of the root system to the drying, that are not taken into account. We argue that, as we assume that root water uptake controls transpiration with this radial approach and our hypothesis, the results qualitatively reproduce several specific types of plant behaviours during the drying period without introducing empirical parameters. Furthermore, the above remarks about phenomena that are not taken into account during water uptake by roots and that can influence the interpretations, could be incorporated into the model provided they are quantified. The second way to justify the use of this model is the accessibility of the inputs of the model (climatic demand, soil hydrodynamic characteristics and root system description). The simplicity of the measurements maintain the operational aspect necessary for the field of agronomy and water management, and yet the model examines complex soil-plant-atmosphere interactions in detail.

The results presented under field conditions (Figs. 9 and 10) show the predictive capacity of the model to reproduce the evolution of soil water content. It is not a validation of the processes incorporated in the model, in the strict sense. From this perspective of process validation, we would suggest

working in a controlled environment system where the root system is perfectly described as well as the soil characteristics: the recent experimental work in the rhizotron and growth chamber and the models of root architecture [4, 24, 65] could quantitatively specify the zone of root water uptake, and could verify the simplifications concerning the homogeneous root water potential. Complementary work on stomatal regulation in response to the root water potential should reveal the links between root absorption, water storage in the plant tissue and transpiration. A second work is envisaged in order to verify and validate the mechanism necessary to model water transfer in the soil-plant-atmosphere continuum.

5. CONCLUSIONS

Some varieties of models exist to describe water transport in the soil-root system. The main objective of this study is to incorporate the mechanisms of soil water transport that can influence plant functioning into a model. The combination of vertical transport and radial diffusion constitutes a new approach towards obtaining an operational model of water uptake by plants. These “microscopic” and “macroscopic” approaches both indicate the role of water soil diffusion around the roots on the entire root system in space.

The characterisation of plant responses to soil water for various types of soil depends on the determination of the limits of extractable soil water. The model introduces water transfer between soil and roots from a physical point of view and it outlines soil drying around the roots and its impact on real transpiration. Consequently, the model seems to be helpful for describing crop behaviour in relation to the combination of soil characteristics, climatic demand and soil exploration by roots. It takes into account the influence of the root system (root length density and radius), soil characteristics (hydrodynamic parameters, vertical water profile) and atmospheric environment (transpirative demand). It introduces the idea that plant regulation could be influenced by the physical soil-root transfer and that threshold root potential (“wilting point”) is a simplified parameter that should be improved including biophysical limits in the plants. For the moment, the approach proposed for calculating the root water potential is used for modelling the initiation of water transport in the plant. It is the first step before taking into account biological regulations of water transfer in the plant such as cavitation, plant capacitance, or the stomatal response to the leaf water potential or to root signalling mechanisms (abscisic acid, for example).

APPENDIXES

A- NUMERICAL DISCRETISATION

Vertical transfer is described in equation (3) and some differences appear for the radial system. The equation of diffusion for the radial flow of water to a cylindrical root is

developed in equation (4). This equation can be simplified by the substitutions [48]:

$$C^* = r \cdot C(\Psi) \text{ and } K^* = r \cdot K(\Psi) \quad (12 \text{ a, b})$$

which lead to the following equation for cylindrical symmetry (Eq. (3) without gravity):

$$C^* \cdot \frac{\partial \Psi}{\partial t} = \frac{\partial}{\partial r} \left[K^* \cdot \frac{\partial \Psi}{\partial r} \right]. \quad (13)$$

So, we use the same discretisation in the space-time grid to solve equations (3) and (13). Space for the transfers is divided into several nodes represented by points z_k with the time step t_j to t_{j+1} . Water fluxes are calculated at the boundary between layers whereas variables are calculated at the node located within these layers. A fully implicit form in time is used. So, the result for the vertical and radial axis is:

$$\frac{\Psi_k^{t_{j+1}} - \Psi_k^{t_j}}{\Delta t} = \frac{1}{C_k^{t_{j+1}}} \frac{1}{\Delta z_k} \left\{ K_{k+1/2}^{(t_{j+1})} \frac{\Psi_{k+1}^{t_{j+1}} - \Psi_k^{t_{j+1}}}{\Delta z_{k+1/2}} - K_{k-1/2}^{(t_{j+1})} \frac{\Psi_k^{t_{j+1}} - \Psi_{k-1}^{t_{j+1}}}{\Delta z_{k-1/2}} \right\}. \quad (14)$$

Of course, for the vertical axis, the term $\left[-\frac{1}{C_k^{t_{j+1}}} \frac{1}{\Delta z_k} \cdot (K_{k+1/2}^{(t_{j+1})} - K_{k-1/2}^{(t_{j+1})}) \right]$ is added to this equation and, for the radial axis, the terms K and C must be substituted by K^* and C^* [Eq. (12 a, b)]. The description of this equation is given for points (z_k, t_j) in the range $0 \leq z \leq \max \text{depth}$ for the vertical axis and $R_{\text{root}} \leq r \leq \text{HMRD}(z)$ for the radial axis with arbitrary nodes k ($k = 0, 1, \dots, n_v$ for the vertical axis; $k = 0, 1, \dots, n_r$ for the radial axis; $j = 0, 1, \dots, n_t$ for time). Precise information grouped in table III must be given concerning the above finite differences.

Internodal conductivities are calculated by geometric means [39] for the vertical and radial systems:

$$K_{k+1/2}^{(t_{j+1})} = \left(K_k^{(t_{j+1})} \times K_{k+1}^{(t_{j+1})} \right)^{1/2} \quad \text{and} \quad K_{i+1/2}^{*(t_{j+1})} = \left(K_i^{*(t_{j+1})} \times K_{i+1}^{*(t_{j+1})} \right)^{1/2}. \quad (15)$$

Since this paper concentrates on water extraction, a null flux condition at the surface and at the bottom limit is imposed for the vertical axis. For water extraction, a Dirichlet condition at the soil-root interface is prescribed because we assume that root water potential is the driving force behind water uptake. Because of symmetry, at the outer boundary of the soil cylinder, a Neumann condition is imposed. The flux condition requires a virtual node outside the domain and makes it possible to impose a flux equal to zero.

The numerical technique for finite difference using a fully implicit form leads to n_r differential coupled and non-linear equations for each radial system and n_v for the vertical system. For each equation, the unknown variable is the water potential in the node k for time t_{j+1} ($t + \Delta t$). The system is solved using a

Gaussian elimination method. The stability of this form of resolution is established in Carnahan [12] and the implicit form used is approximated using an iterative recursive process until the following criterion is satisfied:

$$\text{For } k = 0, \dots, n_r \text{ or } k = 0, \dots, n_v: \quad (16)$$

$$\left| \frac{(\Psi_k^{t_{j+1}})^h - (\Psi_k^{t_{j+1}})^{h+1}}{(\Psi_k^{t_{j+1}})^h} \right| < \varepsilon_c$$

with h , iterative process number “ h ” and ε_c a relative error threshold. If h is equal to zero, the resolution results in an explicit scheme. This first initialisation makes it possible to calculate the terms $K^{(t_{j+1})}$ and $C^{(t_{j+1})}$. So we test the convergence of the implicit form for $1 \leq h \leq 4$. This algorithm is used to control the time step Δt during the calculation. Δt is divided by 2 if more than 4 iterations are necessary to satisfy the criterion ε_c . The stability is also tested by the decrease in error for the mass balance with the decrease in Δt .

In the model, there is one radial system for each horizontal layer. The resolution of each radial system is carried out before the resolution of the vertical system, as explained in Section 2.1.3.

B- LIMITING FLUX FOR ROOT EXTRACTION

B-(a) Why a limiting flux? (analysis in steady state case)

For a steady state, which is used by many authors to describe water extraction, the limit of root extraction [49, 84] depends on the hydraulic properties of the soil. Water soil extraction by the following equation is expressed by:

$$q_r = \frac{2\pi}{\ln\left(\frac{HMRD}{R_{root}}\right)} \int_{\Psi_{root}}^{\Psi_{HMRD}} K(\Psi) \cdot d\Psi. \quad (17)$$

This equation comes from Darcy's law and shows the rate of root uptake per unit length of root (q_r in $\text{m}^2 \cdot \text{s}$) which is correlated to the root water uptake from each root per unit length of root ($\phi = \rho_w \cdot q_r$ in $\text{kg} \cdot \text{m}^{-1} \cdot \text{s}^{-1}$). This equation

indicates the Kirschhoff potential Φ [$\Phi(\Psi_\lambda) = \int_{-\infty}^{\Psi_\lambda} K(\Psi) \cdot d\Psi$].

So, equation (17) becomes:

$$q_r = \frac{2\pi}{\ln\left(\frac{HMRD}{R_{root}}\right)} \cdot (\Phi(\Psi_{HMRD}) - \Phi(\Psi_{root})). \quad (18)$$

As hydraulic conductivity tends towards zero when the soil becomes very dry, we can argue that $\Phi(\Psi_{root})$ becomes negligible before $\Phi(\Psi_{HMRD})$ and so an upper limit appears for the flux from soil to root. An expression of this limiting flux is obtained from equation (18) by setting Ψ_{root} at minus infinity.

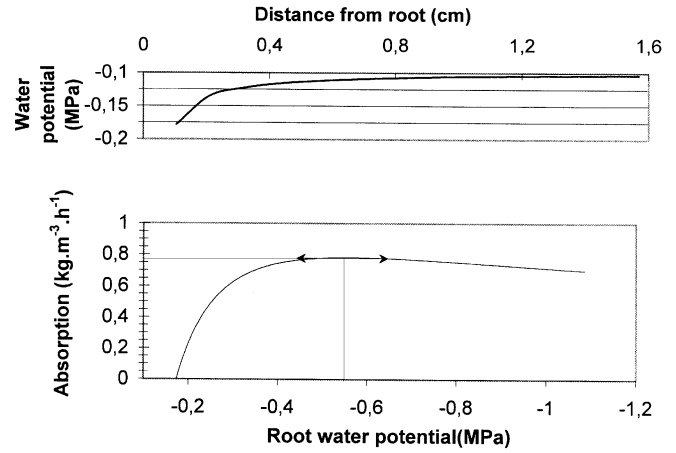


Figure 11. (A) Representation of the initial radial profile used for tests (at t). This radial profile comes from a previous simulation with silt soil. (B) Representation of root water uptake (influx) according to the root water potential at the soil-root interface. Soil used is silt soil (Tab. I), length root density is defined with distance between roots (A), initial radial profile is given in A.

$$q_r^{\text{lim}} = \frac{2\pi}{\ln\left(\frac{HMRD}{R_{root}}\right)} \cdot \Phi(\Psi_{HMRD}). \quad (19)$$

In this situation, water extraction cannot exceed a limit value dependent on the boundary of the soil cylinder ($HMRD$ and R_{root}) and on the relationship between the water potential and hydraulic conductivity relationship ($K(\Psi)$).

B-(b) What situation for numerical resolution?

In keeping with equation (14), the flux at the inner boundary of the radial space system is expressed in equation (20).

$$q_r = K_{\text{interface}}^* \cdot \left(\frac{\partial \Psi}{\partial r} \right)_{\text{interface}}. \quad (20)$$

This flux q_r ($\text{m}^2 \cdot \text{s}^{-1}$) corresponds to water transfer from the soil to the root interface located at $R_{root}(\Psi_{root})$ at time t . The decrease in Ψ_{root} leads to a decrease in internodal conductivity $K_{\text{interface}}^*$ and an increase in the potential gradient between the soil and soil-root interface. At time t , according to the decrease in conductivity, an extremum for the water flux can appear because of the combination of the decrease in conductivity and the increase in the internal potential (Ψ_{root}).

Numerical resolution for radial water transfer in a radial space grid allows us to outline this limiting value of the water uptake (Fig. 11). From an initial radial moisture profile at t , the absorbing water flux (ϕ) is given for various Ψ_{root} values imposed at the inner boundary condition during Δt . The water flux is calculated by the variation in water mass during Δt . Figure 11 shows the extremum of the uptake function. It is characterised by a minimal root water potential and a maximum water influx. This extremum shows that water transfer from soil to root cannot exceed a threshold flux for a

given spatial discretisation, type of soil and soil water potential. Obviously, changes to any one of these points will affect the minimal root water potential and threshold flux values.

Thus, in the model, the search algorithm for adjusted root water potential allows us to detect the increase, stagnation or decrease in flux into the root according to the decrease in root water potential since, at each time t (during Δt), a set of Ψ_{root} values is tested in order to adjust water uptake and maximal transpiration.

REFERENCES

- [1] Allen R.G., Ahmad W.I.A., 2-D evaporation and root extraction in an FEM, Proceedings of the Water forum '92, Irrigation and drainage Baltimore, 2-6 August 1992, pp. 189-196.
- [2] Améglio T., Archer P., Cohen M., Valancogne C., Daudet F.A., Dayau S., Cruiziat P., Significance and limits in the use of predawn leaf water potential for tree irrigation, *Plant and Soil* 207 (1999) 155-167.
- [3] Aussenc G., Granier A., Ibrahim M., Influence du dessèchement du sol sur le fonctionnement hydrique et la croissance du Douglas, *Acta Oecol.* 5 (1984) 241-253.
- [4] Bidel L., Renault P., Pagès L., Rivière L.M., An improved method to measure spatial variation in root respiration: application to the taproot of a young peach tree *Prunus persica*, *Agronomie* 21 (2001) 179-192.
- [5] Blizzard W.E., Comparative resistance of the soil plant to water transport, *Plant Physiol.* 66 (1980) 809-814.
- [6] Bouma J., Using morphometric expressions for macropores to improve soil physical analyses of field soils, *Geoderma* 46 (1990) 3-11.
- [7] Braud I., Dantas Antonino A.C., Vauclin M., Thony J.L., A simple soil-plant-atmosphere transfer model (SiSPAT): Development and field verification, *J. Hydrol.* 166 (1995) 231-250.
- [8] Breda N., Garnier A., Barataud F., Moyne C., Soil water dynamics in an oak stand: Soil moisture, water potentials, and water uptake by roots, *Plant and Soil* 172 (1995) 17-27.
- [9] Bristow K.L., Campbell G.S., Calissendorf C., The effects of texture on the resistance within the rhizosphere, *Soil Sci. Soc. Am. J.* 48 (1984) 266-270.
- [10] Bruand A., Cousin I., Nicoulaud B., Duval O., Bégon J.C., Backscattered electron scanning images of soil porosity for analyzing soil compaction around roots, *Soil Sci. Soc. Am. J.* 60 (1996) 895-901.
- [11] Bruckler L., Lafolie F., Tardieu F., Modelling root water potential and soil-root water transport: II. Field comparisons, *Soil Sci. Soc. Am. J.* 55 (1991) 1213-1220.
- [12] Carnahan B., Luther H.A., Wilkes J.O., Approximation of the solution of partial differential equations, *Applied Numerical Methods*, Ed. John Wiley & Sons, New York, London, Sydney, Toronto, 1969.
- [13] Carsel R.F., Parrish R.S., Developing joint probability distributions of soil water retention characteristics, *Water. Resour. Res.* 24 (1988) 755-769.
- [14] Celia M.A., Bouloutas E.T., Zarba R.L., A general mass-conservative numerical solution for the unsaturated flow equation, *Water. Resour. Res.* 26 (1990) 1483-1496.
- [15] Clausnitzer V., Hopmans J.W., Simultaneous modeling of transient three-dimensional root growth and soil water flow, *Plant and Soil* 164 (1994) 299-314.
- [16] Cowan I.R., Transport of water in the soil-plant-atmosphere system, *J. Appl. Ecol.* 2 (1965) 221-239.
- [17] Cruiziat P., Tyree M.T., La montée de la sève dans les arbres, *La Recherche* 220 (1990) 406-414.
- [18] Denmead O.T., Shaw R.H., Availability of soil water to plants as affected by soil moisture content and meteorological conditions, *Agron. J.* 54 (1962) 385-390.
- [19] Dexter A.R., Compression of soil around roots, *Plant and Soil* 97 (1987) 401-406.
- [20] Diggle A.J., ROOTMAP - A model in three dimensional coordinates of the growth and structure of fibrous root systems, *Plant and Soil* 105 (1988) 169-178.
- [21] Dirksen C., Raats P.A.C., Water uptake and release by alfalfa roots, *Agron. J.* 77 (1985) 621-626.
- [22] Doussan C., Pagès L., Vercambre G., Modelling the hydraulic architecture of root systems: an integrated approach to water absorption - Model description, *Ann. Bot.* 81 (1998) 213-223.
- [23] Doussan C., Vercambre G., Pagès L., Modelling the hydraulic architecture of root systems: an integrated approach to water absorption - Distribution of axial and radial conductances in maize, *Ann. Bot.* 81 (1998) 225-232.
- [24] Doussan C., Vercambre G., Pagès L., Water uptake by two contrasting root systems (maize, peach tree): results from a model of hydraulic architecture, *Agronomie* 19 (1999) 255-263.
- [25] Droogers P., van der Meer F.B.W., Bouma J., Water accessibility to plant root in different soil structure occurring in the same soil type, *Plant and Soil* 188 (1997) 83-91.
- [26] Duham R.J., Nye P.H., The influence of soil water content on the uptake of ions by roots: I/ Soil water content gradients near a plane onion roots, *J. Appl. Ecol.* 10 (1973) 585-598.
- [27] Faiz S.M.A., Weatherley P.E., The location of the resistance to water movement in the soil supplying the roots of transpiring plants, *New Phytol.* 78 (1977) 337-347.
- [28] Faiz S.M.A., Weatherley P.E., Root contraction in transpiring plants, *New Phytol.* 92 (1982) 333-343.
- [29] Faiz S.M.A., Weatherley P.E., Further investigations into the location and magnitude of the hydraulic resistance in the soil: plant system, *New Phytol.* 81 (1978) 19-28.
- [30] Feddes R.A., Bressler E., Neuman S.P., Field test of modified numerical model for water uptake by root systems, *Water Resour. Res.* 10 (1974) 1199-1206.
- [31] Feddes R.A., Kowalik P.J., Zaradny H., Simulation of field water use and crop yield, Halsted Press, New York, 1978.
- [32] Ferreira M.I., Katerji N., Is the stomatal conductance in a tomato crop controlled by soil or atmosphere? *Oecologia* 92 (1992) 104-107.
- [33] Gardner W.R., Dynamic aspects of water availability to plants, *Soil Sci.* 89 (1960) 63-73.
- [34] Gardner W.R., Ehlig C.F., Impedance to water movement in soil and plant, *Science* 138 (1962) 522-523.
- [35] Greacen E.L., Farrell D.A., Cockroft B., Soil resistance to metal probes and plant roots, *Trans. Int. Congr. Soil Sci.*, Elsevier, New York Adelaide, 1968, pp. 769-779.
- [36] Hainsworth J.M., Aylmore L.A.G., Non-uniform soil water extraction by plant roots, *Plant and Soil* 113 (1989) 121-124.
- [37] Hamza M.A., Aylmore L.A.G., Soil solute concentration and water uptake by single lupin and radish plant roots. I/ Water extraction and solute accumulation, *Plant and Soil* 145 (1992) 187-196.
- [38] Hanks R.J., Soil evaporation and transpiration. Modelling plant and soil systems, in: Hanks J.R. (Eds.), Madison, Wisconsin USA, 1991, pp. 245-272.
- [39] Haverkamp R., Vauclin M., A note on estimating finite difference interblock hydraulic conductivity values for transient unsaturated flow problems, *Water Resour. Res.* 15 (1979) 181-187.
- [40] Hillel D., Fundamental of soil physics, Academic Press, 1980.
- [41] Hillel D., Talpaz H., van Keulen H., A macroscopic model of water uptake by a nonuniform root system and of water and salt movement in the soil profile, *Soil Sci.* 121 (1976) 242-255.

- [42] Hillel D., van Beek C.G.E.M., Talpaz H., A microscopic-scale model of soil water uptake and salt movement to plant roots, *Soil Sci.* 120 (1975) 386–399.
- [43] Jones M.M., Modelling diurnal trends of leaf water potential in transpiring wheat, *J. Appl. Ecol.* 15 (1978) 613–626.
- [44] Katerji N., Hallaire M., Menoux-Boyer Y., Durand B., Modelling diurnal patterns of leaf water potential in field conditions, *Ecol. Model.* 33 (1986) 183–205.
- [45] Kirkham M.B., Hydraulic resistance of two sorghums varying in drought resistance, *Plant and Soil* 105 (1988) 19–24.
- [46] Kooistra M.J., Schoonderbeeck D., Boone F.R., Veen B.W., Root-soil contact of maize, as measured by thin-section technique: II- Effects of soil compaction, *Plant and Soil* 139 (1992) 119–129.
- [47] Lafolie F., Bruckler L., Tardieu F., Modelling root water potential and soil-root water transport: I. Model presentation, *Soil Sci. Soc. Am. J.* 55 (1991) 1203–1212.
- [48] Lafolie F., Guennelon R., van Genuchten M.T., Analysis of water flow under trickle irrigation: I. Theory and numerical solution, *Soil Sci. Soc. Am. J.* 53 (1989) 1310–1318.
- [49] Lang A.R.G., Gardner W.R., Limitation to water flux from soil to plants, *Agron. J.* 62 (1970) 693–695.
- [50] McCoy E.L., Boersma L., Unger M.L., Akrotanakul S., Towards understanding soil water uptake by plant roots, *Soil Sci.* 137 (1984) 69–77.
- [51] Moldrup P., Rolston D.E., Hansen J.A., Yamaguchi T., A simple mechanistic model for soil resistance to plant water uptake, *Soil Sci.* 153 (1992) 87–93.
- [52] Molz F.J., Water transport in the soil-root system: transient analysis, *Water Resour. Res.* 12 (1976) 805–808.
- [53] Molz F.J., Remson I., Extraction term of soil moisture use by transpiring plants, *Water Resour. Res.* 6 (1970) 1346–1356.
- [54] Monteith J.L., Evaporation and the environment, *Symp. Soc. Exp. Biol.* 19 (1965) 205–234.
- [55] Mualem Y., A new model for predicting the hydraulic conductivity of an unsaturated porous media, *Water Resour. Res.* 12 (1976) 513–522.
- [56] Newman E.J., Resistance to water flow in soil and plant. II/ A review of experimental evidence on the rhizosphere resistance, *J. Appl. Ecol.* 6 (1969) 261–272.
- [57] Nimah M.N., Hanks R.J., Model for estimating soil water, plant and atmospheric interrelations: II- Field test of model, *Soil Sci. Soc. Am. Proc.* 37 (1973) 328–332.
- [58] Nimah M.N., Hanks R.J., Model for estimating soil water, plant, and atmospheric interrelations: I- Description and sensitivity, *Soil Sci. Soc. Am. Proc.* 37 (1973) 522–527.
- [59] Nobel P.S., Alm D.M., Root orientation vs. water uptake simulated for monocotyledonous and dicotyledonous desert succulents by root-segment model, *Funct. Ecol.* 7 (1993) 600–609.
- [60] Nobel P.S., Sanderson J., Rectifier-like activities of roots of two desert succulents, *J. Exp. Bot.* 35 (1984) 727–737.
- [61] North G.B., Nobel P.S., Hydraulic conductivity of concentric root tissues of Agave Deserti Engelm under wet and drying conditions, *New Phytol.* 130 (1995) 47–57.
- [62] Nye P.H., Tinker P.B., Solute movement in the soil-root system, University of California Press, Berkeley and Los Angeles, 1977.
- [63] Pagès L., Doussan C., Vercambre G., Bruckler L., Habib R., Relation sol-plante et absorption hydrique, *Traité d'irrigation*, in: Thiercelin J.R. (Ed.), Editions techniques et Documentations, Lavoisier Paris, 1998, pp. 88–112.
- [64] Pagès L., Jordan M.O., Picard D., Simulation of the three dimensional architecture of the maize root system, *Plant and Soil* 119 (1989) 147–154.
- [65] Pagès L., Asseng S., Pellerin S., Diggle A., Modelling root system growth and architecture, in: Smit A.L., Bengough A.G., Engels C., Van Noordwijk M., Pellerin S., Van de Geijn S.C. (Eds.), *Root methods, A handbook*, Springer, Berlin, 2000, p. 587.
- [66] Passerat de Silans A., Bruckler L., Thony J., Vauclin M., Numerical modelling of coupled heat and water flows during drying in a stratified bare soil. Comparison with field observation, *J. Hydrol.* 105 (1989) 109–138.
- [67] Passioura J.B., Water transport in and to roots, *Annu. Rev. Plant Physiol. Plant Mol. Biol.* 39 (1988) 245–265.
- [68] Perrier A., Étude physique de l'évapotranspiration dans les conditions naturelles. III : Évapotranspiration réelle et potentielle des couverts de végétaux, *Ann. Agron.* 26 (1975) 229–243.
- [69] Perrier A., Tuzet A., Approche théorique du continuum sol-plante-atmosphère, *Traité d'irrigation*, in: Thiercelin J.R. (Ed.), Editions Techniques et Documentations, Lavoisier, Paris, 1998, pp. 112–146.
- [70] Personne E., Modélisation de la variabilité spatio-temporelle du continuum sol-plante-atmosphère. Cas des couverts bistrates hétérogènes et épars, Ph.D. Thesis, INA PG, Paris, France, 1998.
- [71] Personne E., Tuzet A., Perrier A., Modeling the water consumption of the sparse canopy: Operational approach, in: Brebbia C.A., Anagnostopoulos P., Katsifarakis K., Cheng A.H.D. (Eds.), *Water Resources Management*, WIT Press, Southampton, 2001, pp. 249–257.
- [72] Prasad R., A linear root water uptake model, *J. Hydrol.* 99 (1988) 297–306.
- [73] Reicosky D.C., Kaspar T.C., Taylor H.M., Diurnal relationship between evapotranspiration and leaf water potential in field-grown soybeans, *Agron. J.* 74 (1982) 667–673.
- [74] Reicosky D.C., Ritchie J.T., Relative importance of soil resistance and plant resistance in root water absorption, *Soil Sci. Soc. Am. J.* 40 (1976) 293–297.
- [75] Rice R.C., Diurnal and seasonal soil water uptake and flux within a bermudagrass root zone, *Soil Sci. Soc. Am. Proc.* 39 (1975) 394–398.
- [76] Richards L.A., Capillary conduction of liquids in porous media, *Physics* 1 (1931) 318–333.
- [77] Rieger M., Daniell J.W., Leaf water relations, soil-to-leaf resistance, and drought stress in Pecan seedlings, *J. Am. Soc. Hort. Sci.* 113 (1988) 789–793.
- [78] Rose C.W., Stern W.R., Determination of withdrawal of water from soil by crop roots as function of depth and time, *Aust. J. Soil Res.* 5 (1967) 11–19.
- [79] Schmidhalter U., The gradient between pre-dawn rhizoplane and bulk soil matric potentials, and its relation to the pre-dawn root and leaf water potentials of four species, *Plant Cell Environ.* 20 (1997) 953–960.
- [80] Schmidhalter U., Selim H.M., Oertli J.J., Measuring and modeling root water uptake based on Chloride discrimination in a silt loam soil affected by ground water, *Soil Sci.* 158 (1994) 97–105.
- [81] Scholander P.F., Hammel H.T., Bradstreet E.D., Hemmingser E.A., Sap pressure in vascular plants, *Science* 143 (1965) 339–346.
- [82] Simonneau T., Habib R., Water uptake regulation in peach trees with split root systems, *Plant Cell Environ.* 17 (1994) 379–388.
- [83] Slatyer R.O., *Plant-Water Relationships*, Academic Press, London, 1967.
- [84] Sperry J.S., Adler F.R., Campbell G.S., Comstock J.P., Limitation of the plant water use by rhizosphere and xylem conductance: results from a model, *Plant Cell Environ.* 21 (1998) 347–359.
- [85] Sperry J.S., Pockman W.T., Limitation of transpiration by hydraulic conductance and xylem cavitation in *Betula Occidentalis*, *Plant Cell Environ.* 16 (1993) 279–287.
- [86] Steinhardt R., Ehlers W., van der Poeg R.R., Analysis of soil-water uptake from a drying loess soil by an oat crop using a simulation model, *Irrig. Sci.* 2 (1981) 237–258.
- [87] Steudle E., Water transport across roots, *Plant and Soil* 167 (1994) 79–90.
- [88] Stirzaker R.J., Passioura J.B., The water relations of the soil-root interface, *Plant Cell Environ.* 19 (1996) 201–208.

- [89] Tamari S., Bruckler L., Halbertsma J., Chadoeuf J., A simple method for determining soil hydraulic properties in the laboratory, *Soil Sci. Soc. Am. J.* 57 (1993) 642–651.
- [90] Tardieu F., Bruckler L., Lafolie F., Root clumping may affect the root water potential and the resistance to soil-root water transport, *Plant and Soil* 140 (1992) 291–301.
- [91] Tinker P.B., Roots and water. Transport of water to plant roots in soil, *Philos. Trans. R. Soc. London B* 273 (1976) 445–461.
- [92] Tuzet A., Wilson J.D., Wind and turbulence in a sparse but regular plant canopy, *J. Appl. Meteorol.* (2002) in press.
- [93] Van Bavel C.H.M., Lascano R.J., Stroosnijder L., Test and analysis of a model of water use by sorghum, *Soil Sci.* 137 (1984) 443–456.
- [94] Van Genuchten M.T., A closed-form equation for predicting the hydraulic conductivity of unsaturated soils, *Soil Sci. Soc. Am. J.* 44 (1980) 892–896.
- [95] Veen B.W., Van Noordwijk M., De Willigen P., Boone F.R., Kooistra M.J., Root-soil contact of maize, as measured by thin-section technique. III. Effects on shoot growth, nitrate and water uptake efficiency, *Plant and Soil* 139 (1992) 131–138.
- [96] Vercambre G., Modélisation de l'extraction de l'eau par une architecture racinaire en condition de disponibilité hydrique non uniforme, Ph.-D. Thesis, INA PG, Paris, 1998.
- [97] Yang S.J., de Jong E., Effect of aerial environment and soil water potential on the transpiration and energy status of water in wheat plants, *Agron. J.* 64 (1972) 574–578.
- [98] Young I.M., Variation in moisture contents between bulk soil and the rhizosheath of wheat (*Triticum aestivum* L. cv Wembley), *New Phytol.* 130 (1995) 135–139.
- [99] Zimmermann U., Meinzer F., Bentrup F.W., How does water ascend in tall trees and other vascular plants? *Ann. Bot.* 76 (1995) 541–545.
- [100] Zur B., Jones J.W., Boote K.J., Hammond L.C., Total resistance to water flow in soybeans: II- Limiting soil moisture, *Agron. J.* 74 (1982) 99–105.